Persistence Landscape of Functional Signal and Its Application to Epileptic Electroencaphalogram Data

Yuan Wang, Hernando Ombao, Moo K. Chung

[1]Department of Biostatistics and Medical Informatics

University of Wisconsin, Madison

[2]Department of Statistics

University of California, Irvine

Abstract

Persistent homology is a recently popular multi-scale topological data analysis framework that has many potential scientific applications, particularly in neuroscience. The method can be effectively applied to yield patterns in nonlinear imaging data that are otherwise undetected by existing mono-scale techniques. Among several persistent homological features, recently proposed persistence landscape is used as a new signal detection method in one-dimensional functional data. For this purpose, weighted Fourier series expansion is used for estimating the functional shape of the data before the persistent landscape is obtained. We utilize the proposed method to study topological differences between electroencaphalogram (EEG) data during pre-seizure and seizure periods in a patient diagnosed with left temporal epilepsy.

Keywords. Functional data analysis, weighted Fourier series, persistent homology, persistence landscape, barcodes, EEG.

1 Introduction

Epilepsy is a neurological disease that affects millions worldwide. The World Health Organization (WHO) figures indicate that approximately nine in one thousand people around the world suffered from epilepsy in 1998 [WHO, 2005] (Figure 1). The Centers for Disease Control and Prevention (CDC) have reported that an estimated one percent of adults in the United States currently suffer from active epilepsy [Kobau et al., 2012]. Researchers are pursuing all possible avenues to gain a better understanding of the disease and its effective prevention. To this end, electroencaphalogram (EEG), which is an important brain imaging modality for understanding the function of the human brain, has gained popular ground in studying epileptic seizures. EEG are indirect measurements of neuronal activity recorded at fixed channels on the scalp. Electrical signals thus registered are compared to ground voltage. Many statistical methods have been developed over the past decades to study the patterns of these nonlinear electrical signals [Jansen et al., 1981, Donoho et al., 1998, Ombao et al., 2001]. The major aim of this study is to push the boundaries further by exploring the topological information buried in multi-channel EEG signals and determine whether topological features of EEG can discriminate signals obtained before and during epileptic seizures for the first time.

Algebraic topology has recently gained an unexpected ground in data analysis despite its abstract nature. Consider a set of points S that have been sampled from a topological space X. We are interested in determining the extent to which the topological structure (homology) of X can be inferred from S. The sample S can be represented as skeletal structures called *simplicial complexes* that depend on some parameter λ. By varying the parameter λ of the simplicial complexes built from S, we can obtain a *filtration*, which is the collection of the nested simplicial complexes. Subsequently the filtration will yield the so-called *barcode* for the respective β_i, which are collections of bars with birth and death times of ith-dimensional homology groups of the filtration as their endpoints. A long bar in a barcode indicates a homology class that persists over a long range of parameter values and therefore corresponds to a large scale geometric feature in X, whereas short intervals in a barcode correspond to noise or inadequate sampling [Carlsson, 2009]. This is the basic idea behind persistent homology, a framework originally introduced in [Edelsbrunner et al., 2000].

Barcodes from persistent homology has already shown its power as a standalone analysis tool for complex nonlinear data [Lee et al., 2011, Chung, 2012]. When distinct features are present in the data structure, barcodes alone may suffice to qualitatively distinguish such features. However, it is not straightforward to quantify or perform statistical inference on barcodes [Chung et al., 2009, Heo et al., 2012, Chung, 2012]. A new topological entity called persistence landscape, which builds landscape-like structures based on barcodes, was recently proposed in [Bubenik, 2012] as an alternative way for statistical inference on barcodes.

In this paper, we explore the use of persistence landscape to study epileptic EEG data in pre-seizure and seizure periods. The proposed application procedure consists of EEG signal processing and subsequent topological analysis. The processing step is based on weighted Fourier series [Chung et al., 2010], which can be shown to be equivalent to a wavelet transform. The amplitude of the smoothed EEG signals provide a natural ground for one-dimensional persistent homology and hence persistence landscape. To the best of our knowledge, this is the first application of persistent homology on EEG data.

2 Methods

We formulate the problem as extracting topological features out of smoothed functional data. The smoothing procedure that we propose is based on weighted Fourier series expansion. Persistent homology and corresponding persistence landscapes are then calculated for the smoothed data.

2.1 Functional Data Estimation by Weighted Fourier Series

Neuroanatomical measurements, such as EEG signals can be modeled in the following functional form:

$$f(p) = \mu(p) + \epsilon(p), p \in \mathcal{M} \subset \mathbb{R}^d, \tag{1}$$

where $\mathcal{M}$ is a compact manifold from which the measurements are obtained, $\mu(p)$ is the underlying real-valued signal at p, $f(p)$ is the observed value at p, and $\epsilon(p)$ is a white noise at p. We can impose realistic assumptions that f comes from $L^2(\mathcal{M})$, the space of square integrable functions on $\mathcal{M}$ equipped with the inner product $\langle f, g \rangle = \int_{\mathcal{M}} f(p)g(p)\, d\lambda(p)$ with respect to the Lebesgue measure λ.

Given a sample $\{(p_1, f(p_1)), \dots, (p_n, f(p_n))\}$, a smoothing estimator $\widehat{\mu}$ of the unknown functional signal μ can be constructed as follows. Our aim is to find the estimator $\widehat{\mu}$ in a functional subspace $\mathcal{H}_k \subset L^2(\mathcal{M})$ spanned by an orthonormal basis $\{\phi_j\}$ that spans $\mathcal{H}_k$:

$$\mathcal{H}_k = \left\{ \sum_{j=0}^{k} \beta_j \phi_j(p) : \beta_j \in \mathbb{R} \right\}$$

for some fixed k. The orthonormal basis $\{\phi_i\}$ is given as the eigefunctios of a self-adjoint operator $\mathcal{L}$ defined on $\mathcal{M}$, i.e. $\mathcal{L}\phi_j = \lambda_j \phi_j$ with the eigenvalues $0 \leq \lambda_0 \leq \lambda_1 \leq \lambda_2 \leq \cdots$. Note that the usual Fourier series estimator of μ is given by the shortest distance from f to $\mathcal{H}_k$:

$$\widehat{\mu}(p) = \arg\min_{\mu \in \mathcal{H}_k} ||f - \mu||^2 = \arg\min_{\mu \in \mathcal{H}_k} \int_{\mathcal{M}} |f(p) - \mu(p)|^2 d\lambda(p) = \sum_{j=0}^{k} f_j \phi_j(p),$$

where $f_j = \langle f, \phi_j \rangle$ are the Fourier coefficients.

A weighted version of the Fourier series estimator is used in the current study to smooth EEG signals. It is obtained by minimizing the distance between f and $\mathcal{H}_k$ weighted by the positive definite symmetric kernel

$$K(p, q) = \sum_{j=0}^{\infty} \tau_j \phi_j(p) \phi_j(q) \tag{2}$$

of the operator $\mathcal{L}$ for some constants τ_j (Mercer's Theorem [Conway, 1990]). We assume without loss of generality that the kernel K is a probability distribution with $\int_{\mathcal{M}} K(p, q) d\lambda(q) = 1$ for all $p \in \mathcal{M}$. Then the estimator of μ is given by

$$\widehat{\mu}(p) = \arg\min_{\mu \in \mathcal{H}_k} \int_{\mathcal{M}} \int_{\mathcal{M}} K(p, q) |f(q) - \mu(p)|^2 \, d\lambda(q) d\lambda(p). \tag{3}$$

The unique minimizer of (3) is

$$\widehat{\mu}(p) = \sum_{j=0}^{k} \tau_j f_j \phi_j, \tag{4}$$

which can be shown by plugging $\mu(p) = \sum_{j=0}^{k} \beta_j \phi_j(p)$ into (3) and solving a constrained positive semidefinite quadratic program in β_j. The algebraic detail will not be given due to space limitation. The constants τ_j can be identified by substituting (2) into the kernel convolution on the eigenfunction ϕ_j:

$$K * \phi_j(p) = \int_{\mathcal{M}} K(p,q)\phi_j(q)\, d\lambda(q). \tag{5}$$

Since $K * \phi_j(p) = \tau_j \phi_j(p)$, it is now obvious that τ_j and ϕ_j are the eigenvalues and eigenfunctions of the linear operator $f(p) \to K * f(p)$ respectively.

The estimator $\widehat{\mu}$ can take an alternative form if we consider the linear diffusion-like equation over time t under some initial condition

$$\begin{cases} \frac{\partial g(p,t)}{\partial t} & = -\mathcal{L} g(p,t), t \geq 0, p \in \mathcal{M}, \\ g(p,0) & = f(p), \end{cases} \tag{6}$$

where $f(p)$ describes the observed functional data. The weighted Fourier series (WFS)

$$g(p,t) = \sum_{j=0}^{\infty} e^{-\lambda_j t} \lambda_j \phi_j(p) \tag{7}$$

is the unique solution to (6) [Chung, 2012]. It is now clear that $\tau_j = e^{-\lambda_j t}$. This shows WFS is in fact a solution to diffusion-like partial differential equation. Further it can be shown that WFS is in fact equivalent to diffusion wavelets [Kim et al., 2012]; hence, it effectively reduces the Gibbs phenomenon in the Fourier series estimation of data. Figure 2 shows an illustration of the comparison between Fourier series and WFS in a simple smoothing context. The underlying function takes step values 1 and -1 on the intervals $[0, \pi)$ and $[\pi, 2\pi]$ respectively. All series estimation is based on the 50 terms of finite approximation. The weighted Fourier series with bandwidth $\sigma = 0.02$ is a much closer imitation of the step function than the series with bandwidth $\sigma = 0.1$. The discontinuity at π and the two end-points cause the Fourier series to overshoot, whereas the weighted Fourier series is not affected in the same way and significantly reduces Gibbs phenomenon.

In our analysis of EEG signals, the WFS (7) is adapted for 1D functional data. In 1D, we take the usual 1D Laplacian as the self-adjoint operator $\mathcal{L}$ and subsequently Gaussian kernel becomes the kernel K. The corresponding eigenfunctions of $\mathcal{L}$ are then sine and cosine functions. Then 1D functional signal is estimated as

$$\widehat{\mu}(x) = \sum_{j=1}^{k} \sum_{i=1}^{2} e^{-\lambda_j \sigma} \lambda_j \phi_{ji}(x), \tag{8}$$

with the basis functions

$$\phi_{j1}(x) = \sqrt{2}\sin(j\pi x), \phi_{j2}(x) = \sqrt{2}\cos(j\pi x), j = 1, \ldots, k$$

and corresponding eigenvalues $\lambda_j = j^2\pi^2$ for $j \geq 1$. The parameter σ is the bandwidth of the weighted Fourier series that modulates the smoothness of the estimation. Note that (8) is the diffusion wavelet transform.

2.2 Persistent Homology and Barcodes

The connectivity information of a topological space can be summarized by the so-called homology groups and corresponding Betti numbers β_i up to the dimension of the underlying space. The first three Betti numbers β_0, β_1 and β_2 counts the numbers of connected components, tunnels and voids respectively [Hatcher, 2002].

The birth and death times of intervals in a barcode can be also represented on a planar graph called *persistent diagram*. The persistent diagram of a Morse function, which has unique critical points where the Hessian matrix is nonsingular, can be constructed based on its critical values [Chung et al., 2009]. The construction of persistent diagrams for a one-dimensional Morse function is presented here in a non-technical fashion; a technical account of the topic can be found in [Edelsbrunner and Harer, 2010].

For a one-dimensional Morse function $f : X = \mathbb{R} \to \mathbb{R}$, its sublevel sets are given by $X_a = f^{-1}(-\infty, a]$ for fixed values $a \in \mathbb{R}$. It is obvious that $X_{a_1} \subset X_{a_2}$ for $a_1 \leq a_2$. As a increases, disconnected components in the sublevel sets X_a are first created and later merged with younger components. The process can be seen as the *birth* and *death* of disconnected components. We can represent the births and deaths of the topological components by points on the plane. The *ℓ-th persistence diagram* is denoted $Dgm_\ell(f)$ and for an ℓ-dimensional class α, $Dgm_\ell(f)$ contains a corresponding point of the form $x = (b(\alpha), d(\alpha))$. The *persistence* of the point is denoted $pers(x) = d(\alpha) - b(\alpha)$.

Figure 3(a) shows a simple illustration of persistent homology on smoothed data generated by

$$f(x) = x^2 \cos(7\pi x) + N(0, 0.08), \tag{9}$$

where x runs between 0.5 and 1.5. We denote the smoothing estimate $\widehat{f}$. As we move slightly above of a, a component is born. Another component comes into being just above b. Similarly, a third disconnected component is born at c. However, as we move up to d, the components born in the previous two steps are merged together. This follows from the *Elder Rule* in persistent homology: *older components live on at a merging junction* [Edelsbrunner and Harer, 2010]. So we pair c with d. By the same rule, the merged component is then combined with the next youngest component in the sequence when we reach e. So b is paired with e. At f, all the disconnected components merge into one and a is paired with f. This pairing of birth and death of components is represented in a barcode in Figure 3(b), which shows only the change of β_0. Similarly we can plot barcodes for higher order Betti numbers $\beta_1, \beta_2, \cdots$.

2.3 Statistical Inference on Persistence Landscapes

Our aim is to study the persistent homology of EEG signals smoothed by a weighted Fourier series estimator $\widehat{\mu}$. As descriptors of persistent homology, persistent diagram and its equivalent barcode possess useful properties such as stability with respect to several distance metrics. The *Wasserstein distance*

$$W_p(f,g) = \left[\sum_{\ell} \inf_{\gamma_\ell} \sum_{x} ||x - \gamma_\ell(x)||_\infty^p \right]^{1/p}, \tag{10}$$

where $f, g : X \to \mathbb{R}$ are two tame functions with respective persistence diagrams $Dgm_\ell(f)$ and $Dgm_\ell(g)$, the first sum is over all dimensions ℓ, the infimum is over all bijections $\gamma_\ell : Dgm_\ell(f) \to Dgm_\ell(g)$, and the second sum is over all points x in $Dgm_\ell(f)$, was shown by [Cohen-Steiner and Edelsbrunner, 2010] to be stable. [Mileyko et al., 2011] showed that the persistence diagrams under the Wasserstein metric forms a Polish space, i.e. a complete and separable metric space. Mean and variance appropriate for the space are the *Fréchet mean and variance* as defined respectively by the single element to the *Fréchet mean set* of $\mathcal{P}$, $\{f \in PL^p : F_{\mathcal{P}}(f) = Var_{\mathcal{P}}\}$ and $Var_{\mathcal{P}} = \inf_{f \in PL^p} F_{\mathcal{P}}(f)$, where $\mathcal{P}$ is a probability measure on $(PL^p, \mathcal{B})$ with $\mathcal{B} = \mathcal{B}(PL^p)$ being the σ-algebra of Borel sets in PL^p, and $F_{\mathcal{P}} : PL^p \to \mathbb{R}$ is the *Fréchet function* defined by $F_{\mathcal{P}}(f) = \int_{PL^p} ||f - g||_p^2 \mathcal{P}(dg)$.

In [Bubenik, 2012], the concept of *persistence landscape* was introduced to provide a setting for the calculation of Fréchet mean and variance for persistent homology. Given an interval in a barcode (a, b) with $a \leq b$ (or equivalently a birth and death pair (a, b) in the corresponding persistence diagram), we can define the piecewise linear *bump function* $f_{(a,b)} : \mathbb{R} \to \mathbb{R}$ by

$$f_{(a,b)}(t) = \max(\min(t - a, b - t), 0). \tag{11}$$

The *persistence landscape* of $\{(a_i, b_i)\}_{i=1}^n$ is the set of functions $\lambda_k : \mathbb{R} \to \mathbb{R}, k \in \mathbb{N}$ defined by

$$\lambda_k = k\text{th largest value of } \{f_{(a_i,b_i)}(t)\}_{i=1}^n, \tag{12}$$

with $\lambda_k(t) = 0$ for $k > n$. Figure 5 illustrates the idea of persistent landscape for the barcode associated with smoothed data generated by the function (9). Since there is overlap between the barcode components, the right-angled isosceles triangles corresponding to the bump function (11) may cross each other at these overlapping base values (Figure 4(b)). The persistence landscape $\{\lambda_k\}_{k=1,2,3}$ traces the kth outermost outline of these crossover triangles (Figures 5(a)-5(c)). It is obvious that the landscape assumes zero value elsewhere.

After smoothing by WFS, we set out to compare the average persistence landscapes of two smoothed data sets. The measure of difference between two persistence landscapes in the current context is the *p-persistence landscape distance*

$$d_p(M_1, M_2) = ||\lambda(M_1) - \lambda(M_2)||_p, \tag{13}$$

where $\lambda(M) : \mathbb{N} \times \mathbb{R} \to \bar{\mathbb{R}}$ is defined by $\lambda(M)(k,t) = \lambda_k(M)(t)$, was also defined for any two persistence landscapes M_1 and M_2. In actual analysis, we use the 2-persistence distance between the average persistence landscapes $\bar{\lambda}^{n_1}$ and $\bar{\lambda}^{n_2}$ of the two subsampled data sets

$$d_2 = \left(\int \sum_{k=1}^{K} ||\bar{\lambda}^{n_1}(k,t) - \bar{\lambda}^{n_2}(k,t)||^2 dt \right)^{1/2},$$

which we use

$$\left(\sum_{i=1}^{m} \sum_{k=1}^{K} \Delta t_i ||\bar{\lambda}^{n_1}(k,t_i) - \bar{\lambda}^{n_2}(k,t_i)||^2 \right)^{1/2}$$

to approximate, where the $t_i, i = 1, \ldots, m$, are the synchronized intervals of the two sets of landscapes.

Given one sample for each smoothed data set, 10 subsamples were created by pooling functional values at the $(10+s)$th, $s = 1, \ldots, 10$, time points on the span of each data set. Persistence landscapes for these subsamples were calculated for each set of data, so were their average persistence landscapes. The statistical significance of observed difference between two average persistence landscapes under the null hypothesis of

H_0 : the average persistence landscapes come from identical probability distributions,

H_1 : otherwise.

was determined by applying a permutation test a number of times. Permutations were run progressively to monitor convergence.

3 Application to Epileptic EEG Data

EEG measures the electrical potentials generated by the neurons on cerebral cortex. Signals are recorded by electrodes placed on the scalp or intracranially implanted in the patient. A number of systematic techniques have been developed for analyzing EEG signals. A notable parametric method for analyzing univariate EEG during an epileptic seizure was developed in [Jansen et al., 1981]. The method fits autoregressive models to adaptively segmented time-varying spectra and yields parametric estimates for these segments. Despite conceptual compactness, the procedure is computationally intensive and limited. In [Donoho et al., 1998], a model of a locally stationary process was introduced. An adaptive smoothed and consistent estimator of the time-dependent covariance was obtained under the model. The local stationarity idea is based on finding an interval around each time point where the process is approximately stationary. It is the basis of the smooth localized complex exponential (SLEX) method proposed in [Ombao et al., 2001]. The method automatically segments a non-stationary time series into approximately stationary blocks and selects the span for obtaining the smoothed estimates of the time-dependent spectra and coherence.

Epilepsy induces non-stationarity in EEG recording. Our analysis of epileptic seizure EEG signals depends on smoothing by weighted Fourier series and topological analysis by persistent homology. We apply the WFS-based persistence landscape method to an EEG dataset from an epileptic patient. All weighted Fourier smoothing and persistent homology algorithms have been implemented in MATLAB (R2009b, www.mathworks.com). The pairing lemma outlined in [Chung, 2012] for real-valued Morse functions was implemented to obtain the persistence diagrams of weighted Fourier smoothed data.

3.1 Data

The dataset used in the current study was retrieved from a single female subject by the Department of Neurology at the University of Michigan. The female subject was diagnosed with epilepsy on the left temporal lobe. Figure 6 shows a montage of the eight channels at which the EEG signals were sampled at a rate of 100 Hz with a total number of 32,680 time points. Epileptic seizures start at the left temporal site T3 approximately halfway through the recording.

Primary visualization of the eight sets of EEG signals in Figure 7 shows that the pre-seizure period appears to be more stationary than the latter half. Highly volatile oscillations in the seizure period also seem to concentrate in channels located near the T3 channel.

3.2 Results

To obtain balance between computational efficiency and closeness in imitation, the combination of degree $k = 50$ and bandwidth $\sigma = 0.001$ was fixed upon for weighted Fourier smoothing. Figures 8 shows the effect of smoothing on the entire recording span.

Barcodes and their corresponding persistence landscapes are shown in Figures 9 (pre-seizure), 10 (seizure), 11 (pre-seizure) and 12 (seizure). Note that there is a visual difference between the average persistence landscapes of the pre-seizure and seizure periods at each channel. The pre-seizure landscapes are more consistent across multiple folds in the landscape, whereas those obtained during the seizure period appear to be dominated by a single fold in the landscape. This may correspond to the energy patterns before and during epileptic seizure episode. The latter consists of sudden outburst of energy whereas the former constitutes more regularity.

The raw p-value was calculated individually for the 8 channels for the observed d_2 distance between average persistence landscapes to be greater than the shuffled distance based on 2000 permutations

Channel	C3	C4	Cz	P3	P4	T3	T4	T5
p-value	0.247	0.251	0.235	0.25	0.239	0.0005	0.253	0.262

It identifies only one significant site T3, where the patient's epileptic seizure originates. Figure 13 shows plots of 20%, 15%, 10% and 5% lower percentiles of the d_2 distances between average landscapes based on 2000 permutations. It shows convergence in all cases after approximately 500 permutations.

4 Discussion

Weighted Fourier series is a promising approach in functional data estimation. Persistence homology provides an extra layer of data exploration by topological means. The aim of the study was to explore the combined power of the two tools in understanding complex imaging data such as EEG signals. The proposed method was able to identify, completely on its own and without prior information, the left temporal channel (T3) that displayed statistically significant differences between pre-seizure and seizure patterns. It is remarkable that this independent discovery is confirmed by the fact that this patient has left temporal lobe epilepsy and that seizure episodes are often initiated in this region and captured by the T3 channel.

For testing the significance of observed distances between average persistence landscapes, we can also explore the option of parametric test. The d_2 distance may follow a χ^2 distribution under the null hypothesis and the ensuing computation will be much less intensive than the permutation procedure.

References

[Bubenik, 2012] Bubenik, P. (2012). Statistical Topology Using Persistence Landscapes. *arXiv*.

[Carlsson, 2009] Carlsson, G. (2009). Topology and Data. *Bulletin of the American Mathematical Society*.

[Chung, 2012] Chung, M. K. (2012). *Computational Neuroanatomy: The Methods*. World Scientific Publishing Company.

[Chung et al., 2010] Chung, M. K., Adluru, N., Lee, J. E., Lazar, M., Lainhart, J. E., and Alexander, A. L. (2010). Cosine Series Representation of 3D Curves and Its Application to White Matter Fiber Bundles in Diffusion Tensor Imaging. *Statistics and Its Interface*, 3:69–80.

[Chung et al., 2009] Chung, M. M. K., Bubenik, P., and Kim, P. T. P. P. T. (2009). Persistence Diagrams of Cortical Surface Data. In *Information Processing in Medical Imaging*, pages 386–397. Springer.

[Cohen-Steiner and Edelsbrunner, 2010] Cohen-Steiner, D. and Edelsbrunner, H. (2010). Lipschitz Functions Have Lp-Stable Persistence. *Foundations of Computational Mathematics*, 10:127–139.

[Conway, 1990] Conway, J. (1990). *A Course in Functional Analysis*. Springer.

[Donoho et al., 1998] Donoho, D., Mallat, S., and von Sachs, R. (1998). Estimating Covariances of Locally Stationary Processes: Rates of Convergence of Best Basis Methods. Technical report, Department of Statistics, Stanford University, Stanford.

[Edelsbrunner and Harer, 2010] Edelsbrunner, H. and Harer, J. (2010). *Computational Topology*. American Mathematical Society.

[Edelsbrunner et al., 2000] Edelsbrunner, H., Letscher, D., and Zomorodian, A. (2000). Topological Persistence and Simplification. In *Foundations of Computer Science, 2000. Proceedings. 41st Annual Symposium on*, pages 454–463. IEEE.

[Hatcher, 2002] Hatcher, A. (2002). *Algebraic Topology*. Cambridge University Press, Cambridge.

[Heo et al., 2012] Heo, G., Gamble, J., and Kim, P. (2012). Topological Analysis of Variance and the Maxillary Complex. *Journal of the American Statistical Association*, 107(498):477–492.

[Jansen et al., 1981] Jansen, B., Hasman, A., and Lenten, R. (1981). Piecewise analysis of EEGs using AR-modeling and clustering. *Computers and Biomedical Research*, 14(2):168–178.

[Kim et al., 2012] Kim, W. H., Pachauri, D., Hatt, C., Chung, M. K., Johnson, S. C., and Singh, V. (2012). Wavelet Based Multi-Scale Shape Features on Arbitrary Surfaces for Cortical Thickness Discrimination. *Advances in Neural Information Processing Systems (NIPS)*.

[Kobau et al., 2012] Kobau, R., Luo, Y., Zack, M., Helmers, S., and Thurman, D. (2012). Epilepsy in Adults and Access to Care United States , 2010. *Morbidity and Mortality Weekly Report*, 61(45):910–913.

[Lee et al., 2011] Lee, H., Chung, M. K., Kang, H., Kim, B.-N., and Lee, D. S. (2011). Computing the Shape of Brain Networks Using Graph Filtration and Gromov-Hausdorff Metric. In *MICCAI International Conference on Medical Image Computing and Computer-Assisted Intervention*, volume 14, pages 302–9.

[Mileyko et al., 2011] Mileyko, Y., Mukherjee, S., and Harer, J. (2011). Probability Measures on the Space of Persistence Diagrams. *Inverse Problems*, 27(12):1–21.

[Ombao et al., 2001] Ombao, H. C., Raz, J. A., von Sachs, R., and Malow, B. A. (2001). Automatic statistical analysis of bivariate nonstationary time series. *Journal of the American Statistical Association*, 96(454):543–560.

[WHO, 2005] WHO (2005). Atlas: Epilepsy Care in the World. Technical report, World Health Organization.

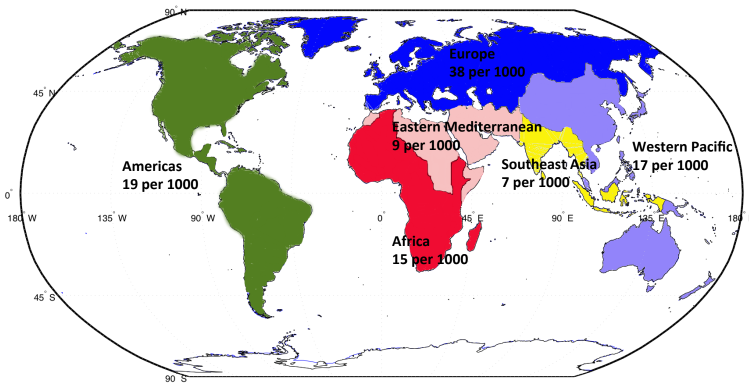

Figure 1: World Health Organization (WHO) figures showing estimated numbers of people around the world suffering from epilepsy in 1998; the world atlas was created using MATLAB (R2009b).

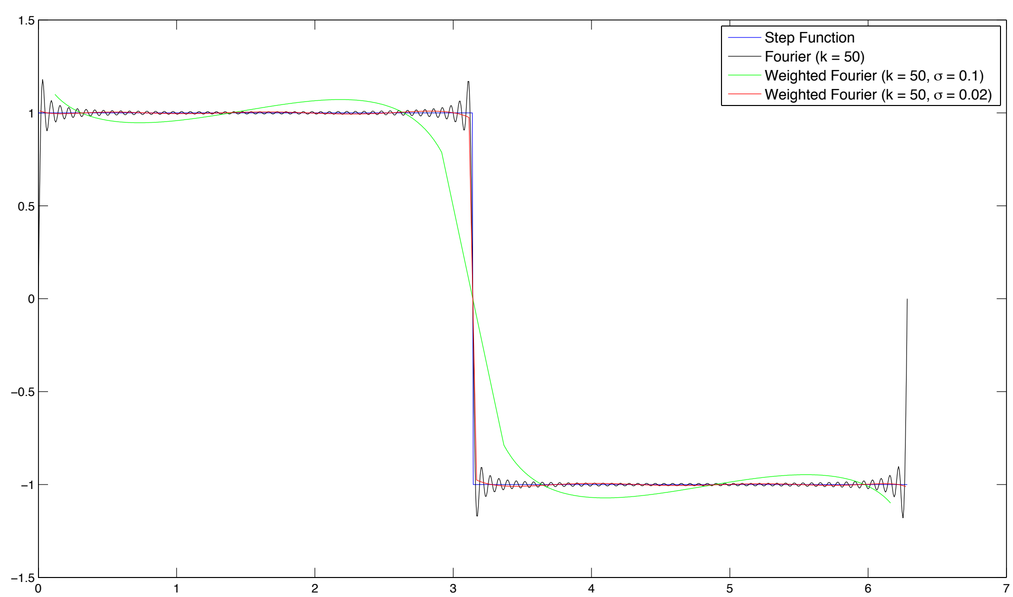

Figure 2: Gibbs phenomenon (ringing artifacts) is visible in the Fourier series expansion of a step function, whereas the weighted Fourier series approximation shows less visible artifacts.

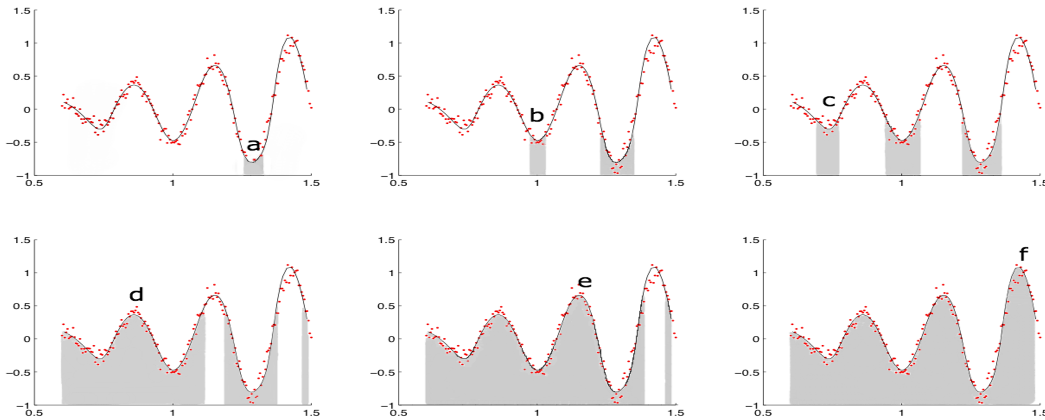

(a) Illustration of Persistent Homology on Smoothed Data.

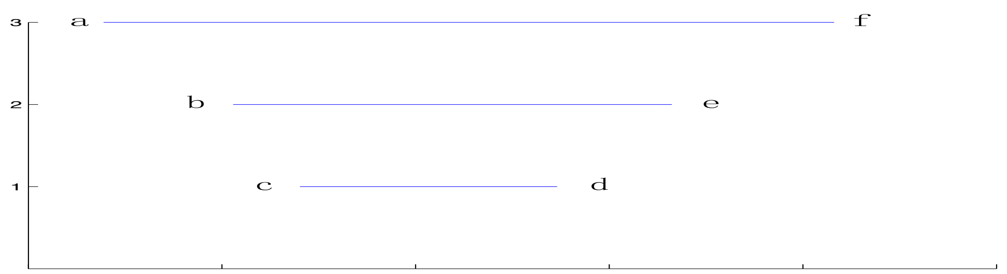

(b) Barcode.

Figure 3: Data generated by function (9) smoothed by a weighted Fourier series with illustration of persistent homology and corresponding barcode showing the birth and death times of path-connected components.

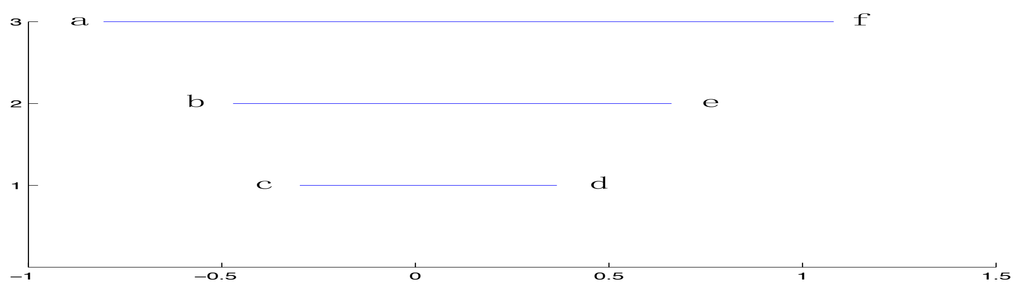

(a) Barcode.

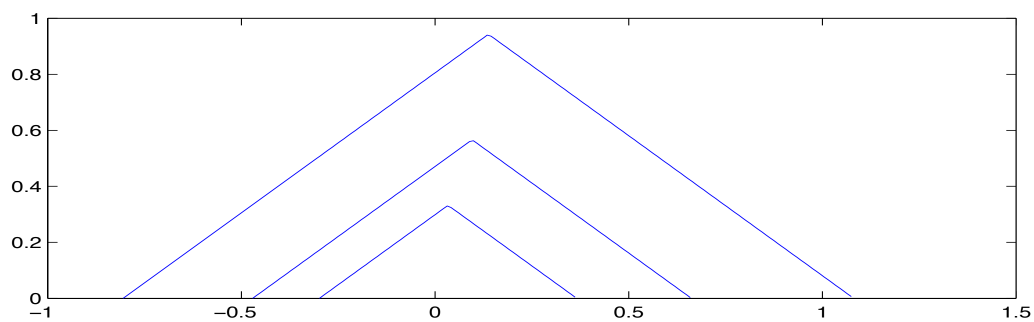

(b) Bump function (11).

Figure 4: A barcode and its corresponding bump function (11).

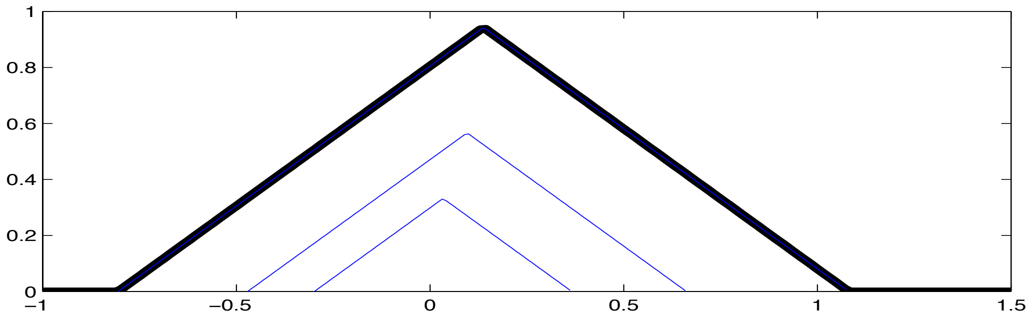

(a) λ_1.

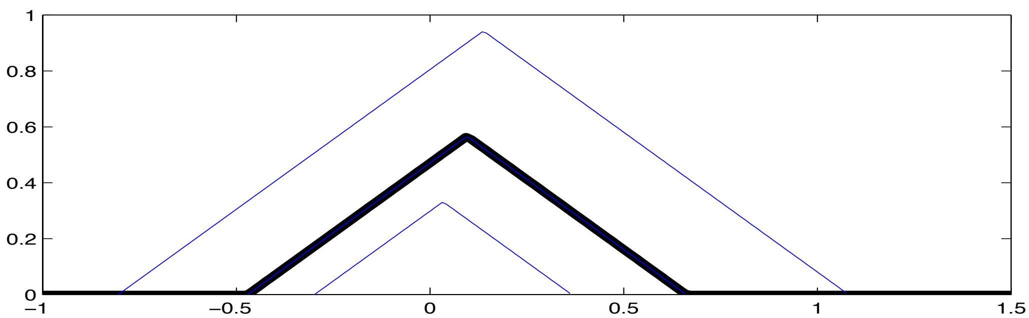

(b) λ_2.

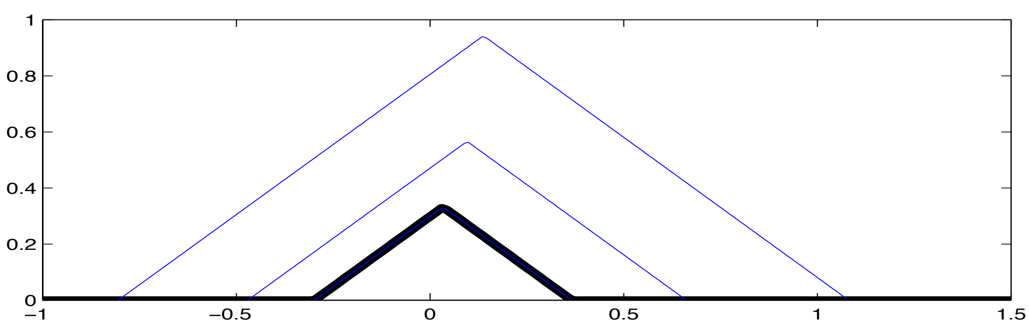

(c) λ_3.

Figure 5: Illustration of persistence landscape.

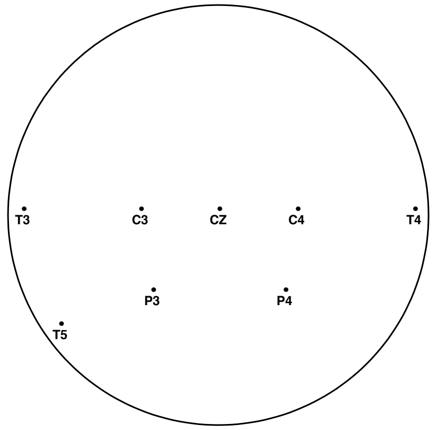

Figure 6: EEG montage with 8 channels in accordance with the international 10-20 system; dots correspond to recording sites; T - temporal, P - parietal, C - central; odd and even numbers indicate left and right hemispheres respectively.

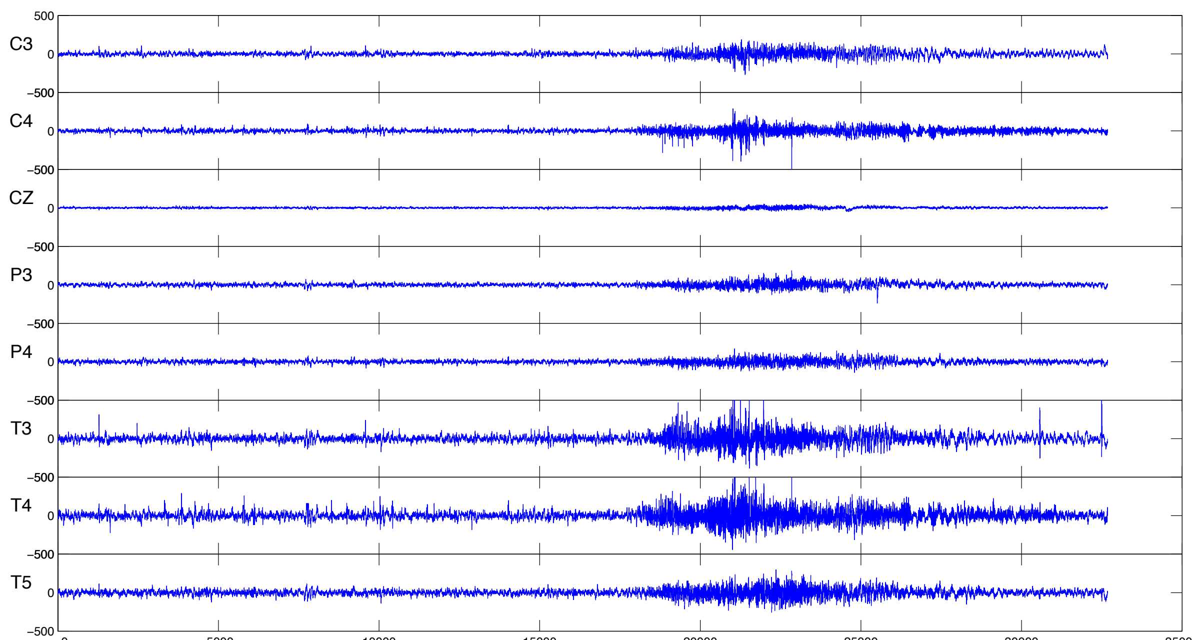

Figure 7: EEG time series at CZ, C3/4, P3/4, T3/4/ and T5; sampling rate of 100Hz with total time points 32,768.

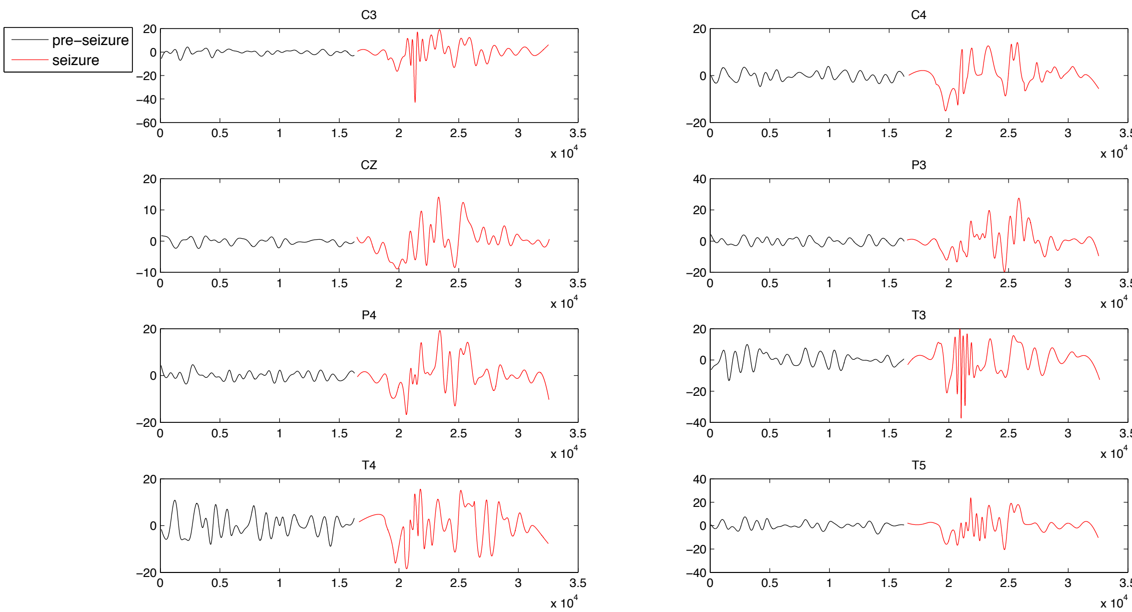

Figure 8: Smoothing by weighted Fourier series of pre-seizure and seizure EEG signals recorded at 8 sites for approximately 3 minutes respectively; degree $k = 50$ and bandwidth $\sigma = 0.001$.

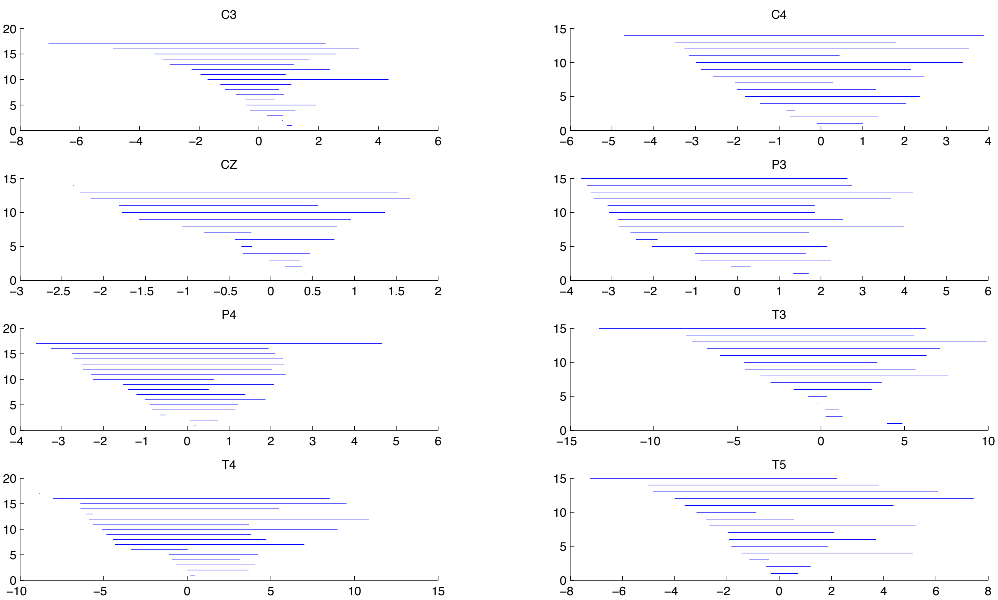

Figure 9: Observed barcodes corresponding to pre-seizure period.

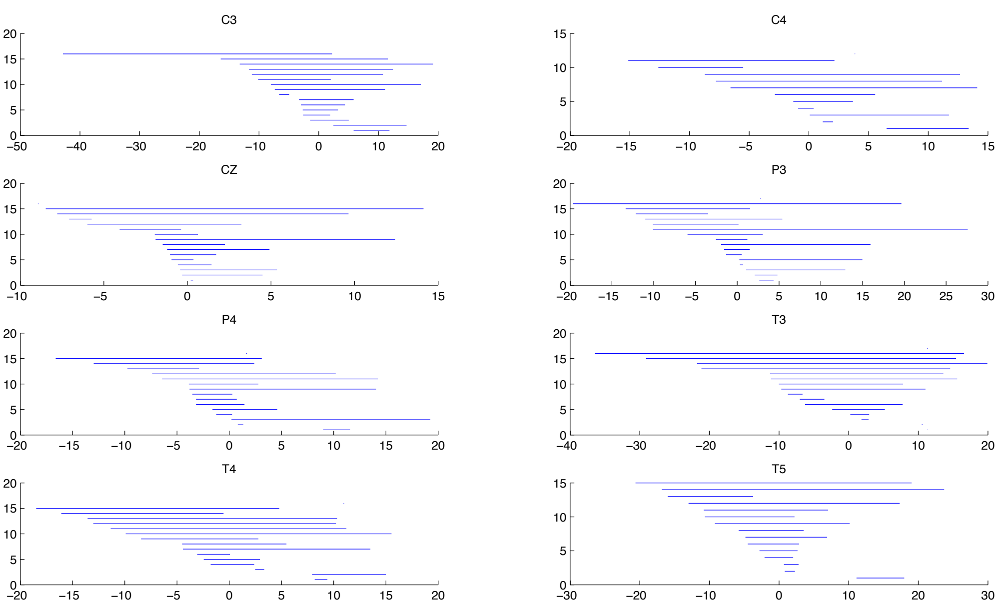

Figure 10: Observed barcodes corresponding to seizure period.

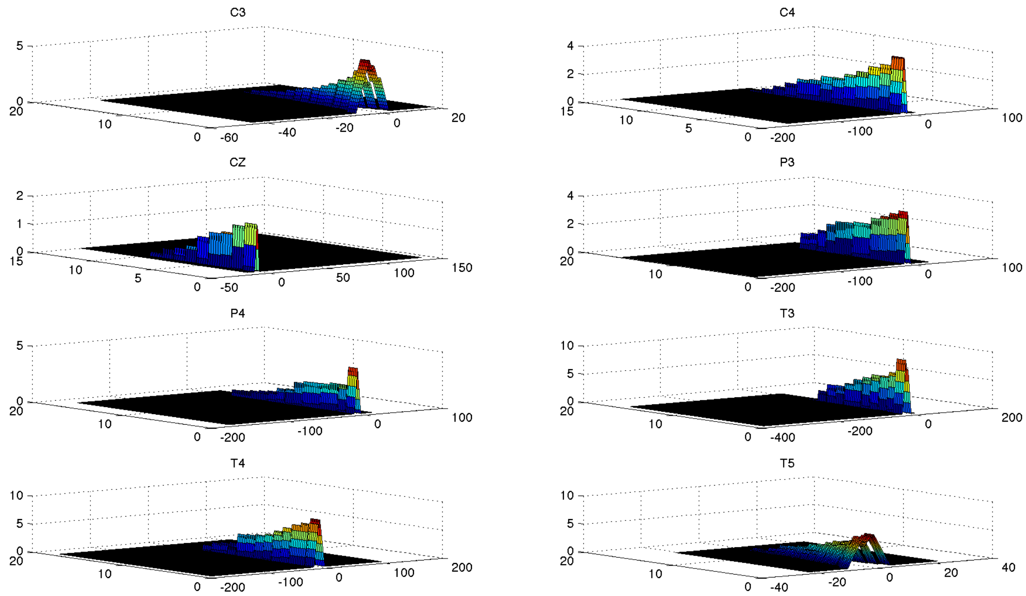

Figure 11: Observed average persistence landscapes corresponding to pre-seizure period.

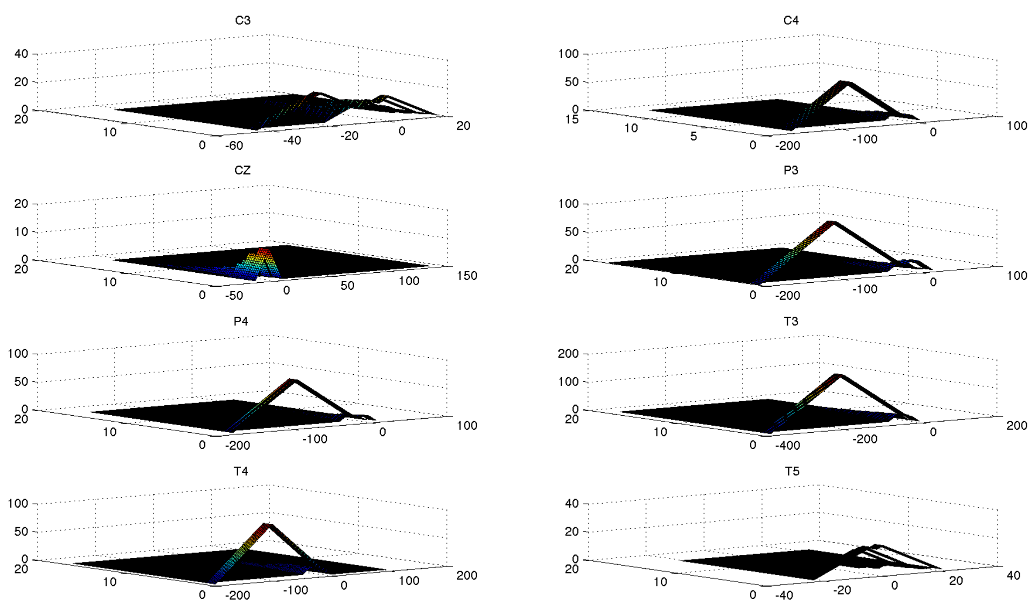

Figure 12: Observed average persistence landscapes corresponding to seizure period.

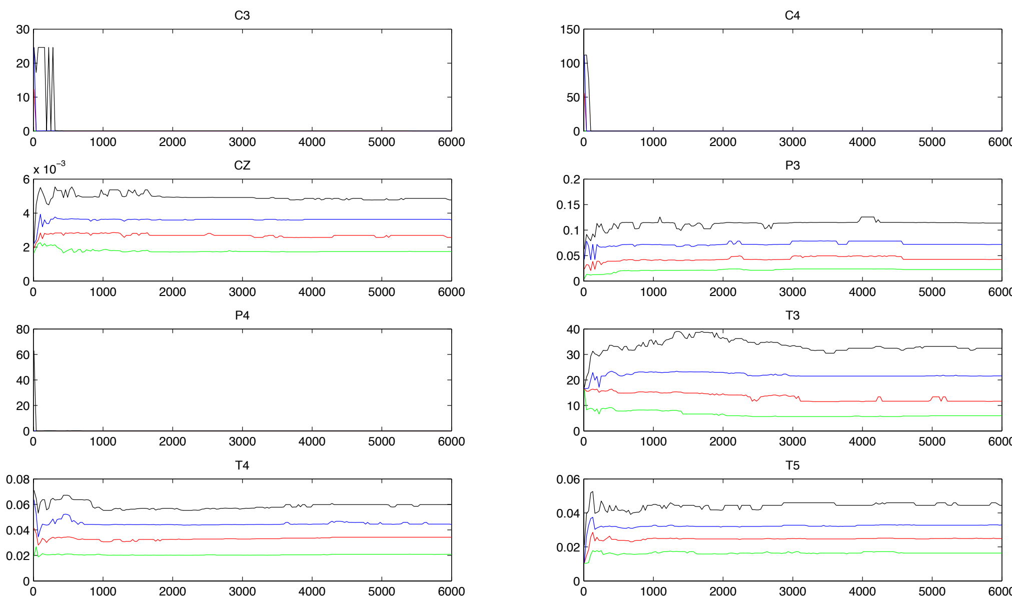

Figure 13: Lower 20% (black), 15% (blue), 10% (red) and 5% (green) percentiles of the d_2 distance between average persistence landscapes based on 2000 permutations